



Regular Article

Noble metal high entropy alloys



Sungwoo Sohn^{a,b}, Yanhui Liu^{a,b}, Jingbei Liu^{a,b}, Pan Gong^c, Silke Prades-Rodel^d, Andreas Blatter^d, B. Ellen Scanley^{b,e}, Christine C. Broadbridge^{b,e}, Jan Schroers^{a,b,*}

^a Department of Mechanical Engineering and Materials Science, Yale University, New Haven, CT 06511, USA

^b Center for Research on Interface Structures and Phenomena, Yale University, New Haven, CT 06511, USA

^c State Key Laboratory of Materials Processing and Die & Mould Technology, Huazhong University of Science and Technology, 1037 Luoyu Road, Wuhan 430074, Hubei, China

^d PX Holding SA, 2304, La Chaux-de-Fonds, Switzerland

^e Department of Physics, Southern Connecticut State University, New Haven, CT 06515, USA

ARTICLE INFO

Article history:

Received 26 May 2016

Received in revised form 18 August 2016

Accepted 18 August 2016

Available online xxxx

Keywords:

High entropy alloys

FCC structure

Solid solution

Compressive property

Phase stability

ABSTRACT

A series of noble metal high entropy alloys with up to six constituent elements has been produced by casting. PtPdRhIrCuNi forms single-phase face-centered cubic solid solution, and its stability is confirmed by annealing experiments. This alloy deforms homogeneously to ~30% to a high ultimate compression strength of 1839 MPa. We discuss rules for the formation of single-phase solid solution.

© 2016 Published by Elsevier Ltd on behalf of Acta Materialia Inc.

In contrast to conventional alloys, which are typically composed of only one or two principal elements, high entropy alloys (HEAs), consist of five or more elements with (near) equiatomic concentration, which form single-phase solid solution (SPSS) [1–5]. This design strategy greatly increases the number of potential technologically relevant alloys [6,7]. The mere combination of practical elements suggests vast numbers of potential HEAs. However, prediction of HEAs out of such vast numbers of potential alloys has been proven to be difficult [6,7]. Predicting stable phases require the knowledge and comparison of the Gibbs free energy of all possible phases [8]. However, this is beyond today's computing power and hence assumptions for ΔH_{mix} and ΔS_{mix} have been suggested [9–12] based on regular mixing behavior [9,10,13–16]. The entropy term has been estimated assuming random configuration contribution at equiatomic composition to $S_c = k \ln n$ (n : number of components) [1]. In the attempt to estimate the enthalpic contribution, pairwise ΔH_{mix} were considered [9,10,14,16,17]. The effect of mixing many elements is estimated through $\Delta H_{\text{mix}} = \sum_{i=1, j=i}^n 4\Delta H_{ij} C_i C_j$ which is the weighted average of all ΔH , the pairwise enthalpy of mixing. For SPSS to form, it has been suggested from empirical considerations [9,10] that this averaged ΔH_{mix} should be in the range from –11.6 to 3.2 kJ/mol [9]. However, deviation from this rule has been

reported [9,11,15,17], suggesting oversimplifications in the estimation of the enthalpic contribution. In addition to thermodynamics, geometric consideration similar to Hume-Rothery has been identified to be crucial in phase formation of HEAs [18,19]. For the formation of solid solutions, it was suggested that the atomic size difference, δ , ($\delta = \sqrt{\sum_i^n C_i (1 - r_i / \sum_i^n C_i r_i)^2} \times 100$, (where r_i is the atomic radius of the i th atom) should be smaller than 6.6% [9].

Considering both thermodynamic and geometrical factors affecting phase formation, we report new HEA systems consisting of noble metals. We found for the noble metals HEAs that, in addition to the weighted average ΔH_{mix} , enthalpy of mixing for individual pairs plays a vital role in phase formation.

We considered Au, Pd, Ag, Pt, Rh, Ir, Cu and Ni for potential alloy constituents. All of the elements are face-centered cubic (FCC) forming elements as listed in Table 1. Binary (AuPd), ternary (AuPdAg), quaternary (AuPdAgPt), quinary (AuPdAgPtCu), and senary (AuPdAgPtCuNi and PdPtRhIrCuNi) alloys at equiatomic composition of approximately 10 g were produced by arc melting of high purity metals. The crystal structure and microstructure of the alloys were studied using X-ray diffraction (XRD) (Rigaku, SmartLab) and scanning electron microscopy (SEM) (Zeiss, Sigma VP) with backscatter electron (BSE). Chemical analysis was performed by using energy-dispersive X-ray spectrum (EDS) attached to SEM. Specimens of dimension of $2 \times 2 \times 4$ mm for compression tests were electric-discharged machined from 3 mm cast samples.

* Corresponding author at: Department of Mechanical Engineering and Materials Science, Yale University, 15 Prospect St BCT, 06520 New Haven, CT, USA
E-mail address: jan.schroers@yale.edu (J. Schroers).

Table 1

Crystal structure, lattice parameter, a , atomic radius, r , and melting temperature, T_m , for considered elements.

	Au	Pd	Ag	Pt	Rh	Ir	Cu	Ni
Structure	FCC	FCC	FCC	FCC	FCC	FCC	FCC	FCC
a , Å	4.078	3.891	4.085	3.924	3.803	3.839	3.615	3.524
r , Å	1.39	1.34	1.37	1.35	1.33	1.35	1.25	1.25
T_m , °C	1064	1555	962	1768	1964	2466	1085	1455

Compression tests were conducted using an Instron mechanical testing machine at a constant strain rate of 10^{-4} s^{-1} .

XRD patterns of the as-cast AuPd, AuPdAg, AuPdAgPt, AuPdAgPtCu, AuPdAgPtCuNi, and PdPtRhIrCuNi alloys are shown in Fig. 1. All peaks have been identified to be solid solutions of FCC structure (space group: $Fm\bar{3}m$). Formation of FCC phases can be expected because all constituent elements are FCC structures, corresponding solid solutions upon solidification at equiatomic composition, and most of the constituent elements have similar physicochemical and thermodynamic parameters (Table 1 and Table S1), such as atomic radii (1.25–1.39 Å), Pauling electronegativity values (1.90–2.54) and valence electron numbers (9–11). Furthermore, for all considered alloys, δ is smaller than 6.6% and ΔH_{mix} is within the range of -11.6 – 3.2 kJ/mol (Table 1).

The XRD patterns exhibit, only one set of FCC diffraction peaks for AuPd, AuPdAg, and AuPdAgPt, suggesting that these alloys form SPSS. However, a second phase of FCC structure forms when Cu is added into AuPdAgPt as demonstrated by the additional set of FCC diffraction peaks in AuPdAgPtCu. Although both δ and ΔH_{mix} remain in the solid solution forming range after Cu addition, pairs of Pt–Cu and Pd–Cu have higher negative enthalpy of mixing compared to the other pairs (Table 2). This indicates that a significant deviation of individual pairs from the average can promote formation of secondary phases. In the attempt to cancel the effect of large negative ΔH from the Pt–Cu and Pd–Cu pairs, we added Ni which has a positive ΔH with Ag and Au (Table 2). This approach however is not successful, a two phase microstructure remains in AuPdAgPtCuNi (Fig. 1). This suggest that a mere consideration of average ΔH_{mix} may be insufficient in predicting SPSS. Instead we considered introducing pairs of moderately positive ΔH by substituting Au and Ag with Rh and Ir (Table 2). As can be seen in Fig. 1, only one FCC phase is present in PdPtRhIrCuNi.

Microstructures observed by SEM-BSE from the central parts of the as-cast samples are shown in Fig. 2(a) and (b) for AuPdAgPtCuNi and PdPtRhIrCuNi, respectively. The AuPdAgPtCuNi alloy shows a microstructure consisting of primary dendrite phases embedded in matrix phases of darker contrast. With length scale ranging from 5 to 10 μm , the dendritic phase is estimated to have a volume fraction about 10 to

Table 2

List of atomic-size difference, δ , enthalpy of mixing, ΔH_{mix} , highest positive enthalpy of mixing ΔH_{max} , and highest negative ΔH_{min} .

Alloys	δ [%]	ΔH_{mix} [kJ/mol]	ΔH_{max} [kJ/mol]	ΔH_{min} [kJ/mol]
AuPd	2.49	0	0	0
AuPdAg	2.33	−5.78	0	−7
AuPdAgPt	2.19	−2.00	4	−7
AuPdAgPtCu	4.25	−6.56	4	−14
AuPdAgPtCuNi	5.39	−2.22	15	−14
PdPtRhIrCuNi	3.71	−2.56	6	−14

20%. These two phases correspond to the two FCC phases in XRD patterns. On the other hand, the single solid solution forming PdPtRhIrCuNi exhibits a completely dendritic microstructure, as shown in Fig. 2(b). The average size of primary arm is about 5 μm . Chemical analyses indicate that the dendrite is Rh and Ir rich, e.g. $\text{Pd}_{48}\text{Pt}_{13}\text{Rh}_{26}\text{Ir}_{34}\text{Cu}_6\text{Ni}_{13}$. The interdendritic region exhibit a varying composition with up to $\text{Pd}_{20}\text{Pt}_{21}\text{Rh}_{13}\text{Ir}_7\text{Cu}_{18}\text{Ni}_{21}$.

In general, there are two possible origins of the compositional variations in the microstructure; non-equilibrium solidification [2] and phase separation [20]. Under a higher diffusive condition, composition gradient should decrease to form a homogeneous SPSS for non-equilibrium solidification and increase for phase separation due to difference in thermodynamic driving force, as schematically illustrated in Fig. 3(a). In order to determine which scenario is present in PdPtRhIrCuNi, we conducted annealing experiments both below and above T_m of the alloy, with the evolution of the element distribution revealed by EDS mapping (Fig. 3(b)–(e)). In the as-cast state (Fig. 3(b)), the distribution of the elements is non-uniform with the dendritic region rich in Rh and Ir and poor in Pd and Cu. When being annealing at 1000 °C (Fig. 3(d)), element distribution becomes more uniform. Further increasing annealing temperature to 1200 °C results in further reduction of composition variations. However, increasing annealing temperature to 1400 °C (Fig. 3(e)) which is above T_s of the alloy, composition variation increases rapidly. To quantify the compositional difference between dendritic and interdendritic regions, we use $\Delta C_{\text{sum}} = \sum |C_{i,\text{bright}} - C_{i,\text{dark}}|$ as an indicator, where i represent the constituent elements so that less difference leads to smaller value of ΔC_{sum} . Fig. 3(f) shows the change of ΔC_{sum} with annealing temperature. The concentration changes for each element can be found in Supplementary Materials. As shown in Fig. 3(b), ΔC_{sum} decreases with increasing annealing temperature from 1000 °C to 1200 °C. At 1400 °C $> T_s$, ΔC_{sum} increases. The changes of ΔC_{sum} with annealing temperature suggest that the compositional variations in as-cast PdPtRhIrCuNi originate from non-equilibrium solidification and the alloy evolves into a homogenous in composition SPSS phase. To confirm if the alloy indeed develops towards a uniform composition FCC SPSS phase, we conducted another set of annealing experiments at constant temperature (1200 °C) for various annealing conditions from 2 h to 200 h, which can be shown in Supplementary Materials. We found that the volume fraction of the bright phase gradually decreases as a function of time [21]. Our results indicate that the microstructure develops towards a homogeneous FCC SPSS phase when approaching equilibrium.

HEAs have been reported to possess a combination of high strength and ductility [4,22]. To evaluate the mechanical property of the PdPtRhIrCuNi, we performed compression tests. As shown in Fig. 4(a), the yield strength, σ_y , of PdPtRhIrCuNi is 527 MPa, while the maximum strength, σ_m , is 1839 MPa. In comparison with previously reported HEAs that form FCC SPSS, the strength of PdPtRhIrCuNi is higher because of the “Cocktail effect” [3], originating especially from the high strength of Rh and Ir. According the stress-strain curve shown in Fig. 4(a), the strain to failure is 32.4%, a value typical for FCC structured HEAs [23]. Fracture appears to occur along the maximum shear stress (Fig. 4(b)). As marked by arrows, numerous slip bands can be observed on sample surface, indicating the homogeneous deformation upon loading. In addition, the data show a dramatic solid-solution-like strengthening

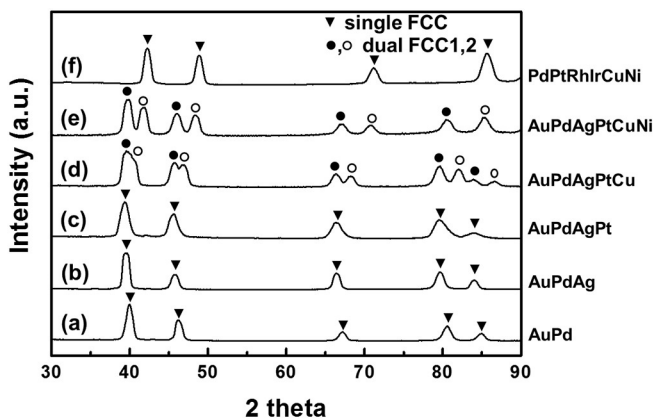


Fig. 1. X-ray diffraction patterns of (a) AuPd, (b) AuPdAg, (c) AuPdAgPt, (d) AuPdAgPtCu, (e) AuPdAgPtCuNi, and (f) PdPtRhIrCuNi.

Download English Version:

<https://daneshyari.com/en/article/1497995>

Download Persian Version:

<https://daneshyari.com/article/1497995>

[Daneshyari.com](https://daneshyari.com)